Poleward intensification of midlatitude extreme winds under warmer climate

npj climate and atmospheric science

www.nature.com/npjclimatsci

ARTICLE OPEN

Check for updates

Poleward intensification of midlatitude extreme winds under warmer climate

Emanuele Silvio Gentile[1]✉, Ming Zhao[2] and Kevin Hodges[3]

Our study investigates the global impact of midlatitude cyclones on extreme wind speed events in both hemispheres under a warmer climate. Using the latest version of the high-resolution ≈ 50 km grid-spacing atmospheric climate model AM4, developed by the Geophysical Fluid Dynamics Laboratory, we conducted simulations covering the 71-years period 1949–2019 for both the present-day climate and an idealised future global warming climate scenario with a homogeneous Sea Surface Temperature (SST) increase by 2 K. Our findings reveal that extreme near-surface wind speeds increase by up to 3% K^{-1} towards the poles while decrease by a similar amount in the lower midlatitudes. When considering only extreme wind speed events objectively attributed to midlatitude cyclones, we observe a migration by the same amount towards higher latitudes both in percentage per degree SST warming and absolute value. The total number of midlatitude cyclones decreases by roughly 4%, but the proportion of cyclone-associated extreme wind speed events increases by 10% in a warmer climate. Finally, Northwestern Europe, the British Isles, and the West Coast of North America are identified as hot spots with the greatest socio-economic impacts from increased cyclone-associated extreme winds.

npj Climate and Atmospheric Science (2023)6:219 ; https://doi.org/10.1038/s41612-023-00540-x

INTRODUCTION

Given the significant risks posed by near-surface extreme wind speeds associated with midlatitude cyclones to lives, livelihoods, and infrastructure[1–4], it is imperative to understand their physical changes, including magnitudes and patterns, under human-induced global climate change. This understanding is crucial for the development of effective climate adaptation strategies and the mitigation of associated risks.

Midlatitude cyclones, often referred to as windstorms, have long been recognized for controlling extreme wind speeds and weather patterns in the midlatitudes[5], and many studies have investigated the response of midlatitude cyclone tracks, intensity, and mesoscale features to a warmer climate in both the NH and the SH[6–13]. In the SH, a consistent and uniform poleward shift of midlatitude cyclone storm tracks has been projected by the end of the 21st century[12,14]. Similarly, in the NH, projections of midlatitude storm tracks in a warmer climate generally showed a poleward shift of storm tracks in the western North Pacific, along with an intensification over the British Isles and Northwestern Europe[15,16], though with less certainty compared with the SH. Moreover, a few recent papers suggest that, under anthropogenic climate warming, the most severe cyclones are expected to further increase in intensity[13,17], though there is no strong consensus[10]. A slightly more robust agreement exist among scientists on the future projections of the overall number of midlatitude cyclones, which are expected to decrease in both hemispheres under a warmer climate[12].

A recent investigation[13] using models from the Sixth Climate Model Intercomparison Project (CMIP6) initiative[18] explored future global changes in extratropical storm tracks, cyclone intensity, wind speed, and structure. The study found a projected reduction of approximately 5% in the number of cyclones by the end of the 21st century, accompanied by a 4% increase in the number of extreme cyclones and higher peak relative vorticity at 850 hPa. These projected changes in cyclone frequency and intensity have implications for the associated wind speeds[6,12]. Specifically, the increase in the number of extreme cyclones, coupled with higher cyclone-associated peak relative vorticity, has been linked to an increase in 850 hPa wind speeds in certain regions of the NH, such as the British Isles and Northwestern Europe[13].

Idealized global warming simulations based on changing the optical thickness of the atmosphere have also indicated potential increases in wind speeds and wind gusts associated with midlatitude cyclones[19]. This effect is likely attributable to the larger latent heat flux associated with warmer climate simulations, which amplifies the positive lower-tropospheric potential vorticity, and this amplification, in turn, enhances cyclone intensity and associated surface winds and gusts[17]. Indeed, results from a single climate model of CMIP6 have demonstrated an increased likelihood of extreme wind speeds in the UK region, attributed to the more frequent occurrence of midlatitude cyclones with sting jets, leading to higher winds and gusts at the surface[20,21]. Similarly, in the SH, simulations from CMIP5 models projected an increase in the wind intensity of extreme winter midlatitude cyclones, aligning with the findings regarding cyclone tracks discussed earlier[12].

Despite the growing attention given in the last decade to future climate projections of midlatitude cyclones and their synoptic and mesoscale characteristics[12,13], there exists a research gap between those studies[12] simulating the response of midlatitude cyclones and associated winds to anthropogenic warming using an idealised modelling set up consisting of an aquaplanet, where either the optical thickness[17] or Sea Surface Temperature (SST)[22] is increased to simulate warmer climates, and those studies investigating climate projections of midlatitude cyclones using the complex fully-coupled CMIP5[9] and CMIP6[13] models. Furthermore, the few studies that have specifically examined how the intensity of the extreme near-surface wind speed events would

[1]Program in Atmospheric and Oceanic Sciences, Princeton University, Princeton, NJ, USA. [2]Geophysical Fluid Dynamics Lab, NOAA, Princeton, NJ, USA. [3]Department of Meteorology, University of Reading and National Centre for Atmospheric Science, Reading, UK. ✉email: emanuelesilvio.gentile@noaa.gov

change have primarily approached the topic from a wind energy perspective[23,24], often disregarding the associated meteorological drivers, e.g., midlatitude cyclones (but also mesoscale convective systems, tropical cyclones...). Both of these research areas have been highlighted by a recent review on the future of midlatitude cyclones as key potential areas for future research directions[12].

In this study, we aim to bridge this research gap by establishing an objective and systematic understanding of the global contribution of midlatitude cyclones to near-surface extreme wind speeds, and how their geographical distribution and intensity may change in the future, using idealised simulations of a warmer climate obtained with a realistic high-resolution general circulation model. Towards this aim, we used the latest GFDL high-resolution, ≈ 50 km grid-spacing, General Circulation Model (GCM), with the Atmospheric Model version 4 (AM4)[25] which has demonstrated its ability to realistically simulate cyclone events, as well as other mesoscale phenomena like tropical storms and mesoscale convective systems[26]. We conducted simulations with the AM4 model spanning the entire 71-year period from 1949 to 2019, for a present-day and a future warmer climate scenario with a homogeneous SST increase of 2 K, which is an idealised representation of anthropogenic climate change[27]. This simulation setup offers the advantage of conducting climate sensitivity experiments with a warmer SST while retaining the benefits of a state-of-the-art climate model, run, and analyzed, at the high resolution of ≈ 50 km grid-spacing. The analysis of the AM4 climate simulations is based on all year data.

RESULTS

Present climate of near-surface extreme wind speeds and associated biases

The present-day climate of extreme near-surface wind speeds and associated biases relative to ERA5 data are depicted in Fig. 1. Figure 1a–b illustrate the median of the 99th-100th percentiles, corresponding to the 99.5th percentile, of the present-day daily maximum 10-m wind speeds (DMWSs) in the NH (Fig. 1a) and in the SH (Fig. 1b), to which we will refer as $v99.5$ in the following text, in the interest of conciseness. It is evident that $v99.5$ exceeds 25 m s^{-1} in both the NH and SH, particularly in regions corresponding to the storm tracks of the North Atlantic[28], North Pacific, and Southern Ocean. However, in the Mediterranean region, where a storm track also exists, the median extreme wind speeds tend to be lower. The discrepancy found in the Mediterranean region may be attributed to the AM4 model resolution of approximately 50 km which may not adequately capture the intense wind speeds associated with the smaller scale of cyclones in this area[29]. Additionally, it may be necessary to adapt the tracking algorithm utilized in this study[30] to effectively detect some of the most intense Mediterranean cyclones, known as medicanes, in future studies that specifically focus on this region[13]. Importantly, the results presented in Fig. 1a–b are skewed towards winter and spring values in both the hemispheres. In fact, when considering only the number of extreme wind speed events occurring during November to March in the NH and during April to September in the SH, they account, respectively, for 71% and 73% of the total extreme wind speed events, making the results in Fig. 1a–b "biased" towards winter and spring seasons.

Before analysing the response of extreme wind speeds to global warming, the major simulation biases of the present climate of extreme wind speeds simulated by the GFDL-AM4 model are presented. Figure 1c–d illustrate the present climate extreme wind speed bias relative to the European Centre for Medium-range Weather Forecasts (ECMWF) fifth generation hourly reanalysis (ERA5)[31], computed as the difference between AM4 and ERA5 $v_{99.5}$. Over the ocean, the AM4 model overestimates the corresponding ERA5 extreme wind speeds up to ≈ 4 m s^{-1}. This could be explained by the higher temporal frequency of the wind-speed timeseries used by AM4 to compute the extreme wind speeds compared to ERA5. In fact, AM4 extreme wind speeds are obtained using DMWS values computed over the daily wind values output every model timestep, 30 minutes, while ERA5 extreme wind speed values are obtained using DMWS computed over the daily hourly mean wind values. Moreover, although both ERA5 and AM4 use the Monin-Obukhov surface layer theory and stability profile functions to estimate the 10-m wind, ERA5 uses an exposure correction approach to make the postprocessed 10-m wind compatible with SYNOP observations. Over inhomogeneous terrain, where the "aerodynamic roughness length" in the model is adjusted to provide sufficient drag at the surface which is dominated by the rough elements, the ERA5 approach corrects the otherwise low area-averaged wind speed, making it comparable with SYNOP observations, which are often taken over an open terrain (as specified by the World Meteorological Organization).

Looking at the present climate biases over land, they are smaller than over the ocean, and contained within ± 2 m s^{-1}, with the exception of regions characterised by high orography, such as Greenland or Antarctica, where AM4 underestimates extreme wind speeds by up to 8 m s^{-1}. Although 10-m hourly winds are not assimilated over land[32], it is plausible that the AM4 model coarser resolution of ≈ 50 km compared to the ERA5 resolution of ≈ 30 km, combined with the lack of an exposure correction method and an excessive orographic gravity wave drag in AM4, explains the large underestimation of AM4 extreme wind speeds over mountainous regions compared to ERA5 values. Therefore, care should be taken when assessing the AM4 future climate projections of extreme wind speeds over high orography regions such as Greenland and Antarctica.

Response of near-surface extreme wind speeds to global warming

The response of extreme wind speeds under the simulated idealised global-warming climate conditions exhibit worldwide spatial variability as depicted in Fig. 2. Figure 2a–b illustrates the projected changes in midlatitude extreme wind speeds under an idealised global warming scenario for both the NH and SH. The results are represented as percentage differences between the warmer and present-day climate simulations of $v99.5$, normalised per sea surface temperature (SST) degree warming. In the NH (Fig. 2a), there is notable increase in extreme wind speeds ranging from 2% to 3% K^{-1} in regions such as the North Atlantic, Western Europe, the west coast of the United States (US), and Canada, spanning latitudes between 50 and 70°N. Conversely, there is a reduction of up to 3% K^{-1} in latitudes between 30 and 50°N. However, the North Pacific exhibits a uniform increase of approximately 2% in extreme wind speeds. The British Isles and Northwestern Europe exhibit the largest increase in extreme wind speeds, both in terms of percentage per SST degree warming (3% K^{-1}) and magnitude (approximately 1.5 m s^{-1}, not shown). This observed increase is similar in magnitude to that projected by the end of the 21st century in a previous study specifically focused on these regions[33]. In the SH (Fig. 2b), a more symmetric pattern of change emerges, with extreme wind speeds projected to increase by up to 3% K^{-1} (approximately 1.5 m s^{-1} in absolute value, not shown) along the entire length of Antarctica, spanning latitudes between 50 and 70°S. Similarly to the NH, regions between 30 and 50°S are expected to experience a decrease of up to 3% K^{-1} in extreme wind speeds, with the exception of the Southern Pacific Ocean region, which shows an increase of up to 2% K^{-1}. To assess whether the difference in the medians $v_{99.5}$ between the present-day and warmer climate distributions resulted from the actual response to +2 K of warming, thus being statistically significant,

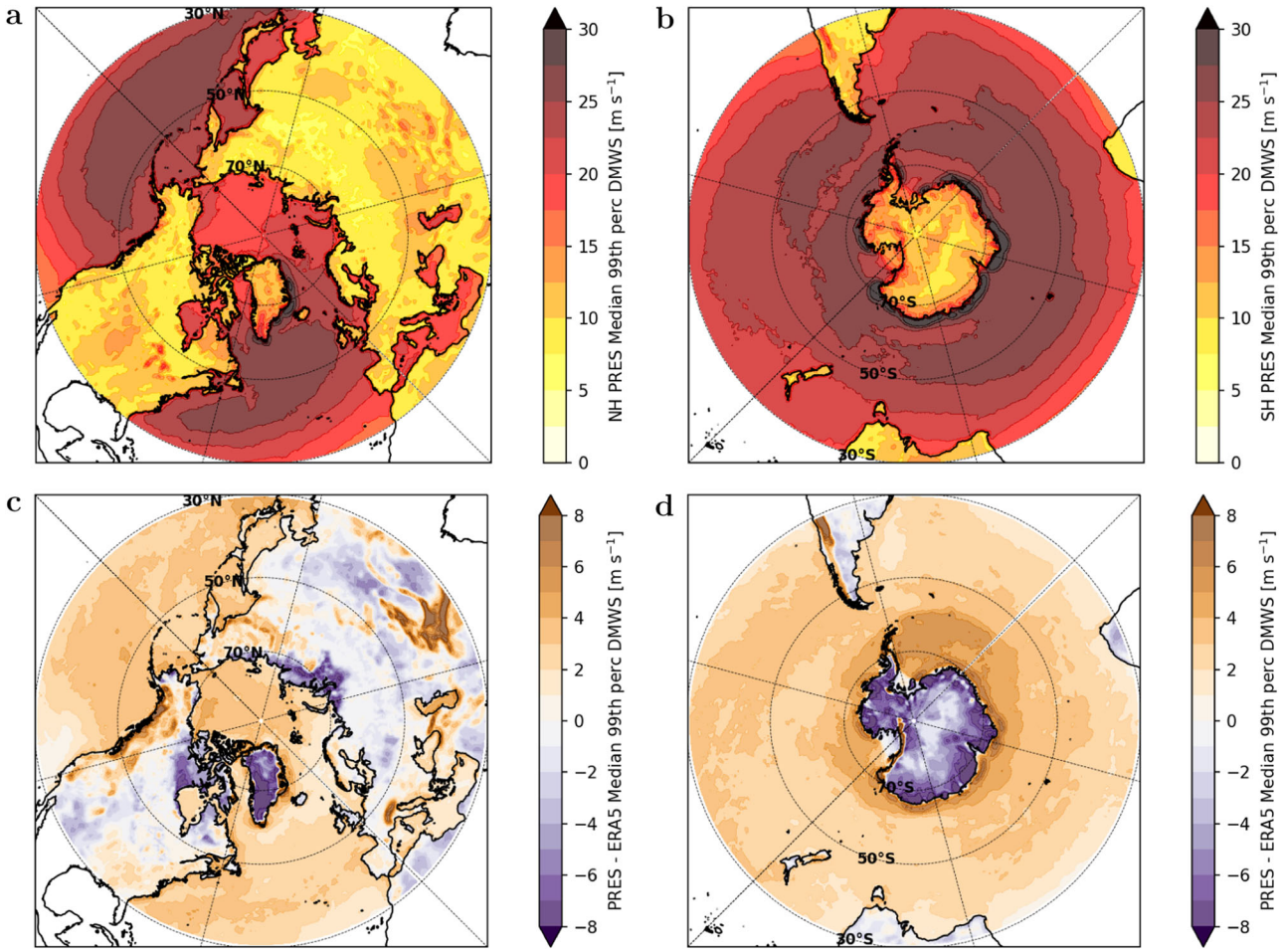

Fig. 1 Map and associated biases of extreme wind speeds in AM4 present-day climate simulations. Spatial distribution of present-day climate simulations for extreme near-surface wind speeds characterised as the median of the 99th-100th percentiles daily maximum 10-m wind speeds (DMWS), corresponding to the 99.5th percentile $v_{99.5}$, in the **a** Northern Hemisphere and **b** Southern Hemisphere. Bias of present-day climate simulations $v_{99.5}$ relative to ERA5 in the **c** Northern Hemisphere and **d** Southern Hemisphere.

rather than merely an outcome of random variations, we applied the non-parametric Mann-Whitney U test to the distributions of extreme DMWSs events in each grid cell for both present and warmer climate simulations. We consistently obtained Mann-Whitney p-values $p < 0.05$ everywhere, indicating the statistical significance of the response to an idealised +2 K SST climate scenario.

These findings suggest a notable and statistically significant poleward migration of extreme wind speeds in both the NH and SH. The poleward migration is more pronounced and consistent in the SH compared to the NH. These results align with previous observations of the shift in midlatitude cyclone tracks under a warmer climate as reported in various studies[6,13,15]. It can be hypothesized that the changing global patterns of midlatitude cyclones play a significant role in driving the changes in extreme wind speeds.

Frequency distribution of cyclone-associated near-surface extreme wind speeds in both present-day and warmer climate simulations

To objectively and systematically evaluate the contribution of midlatitude cyclones to extreme wind speed events, characterized by DMWSs exceeding the 99th percentile threshold, an ad-hoc algorithm is employed in both the present-day and future warming climate simulations.

Figure 3 a presents box plots that summarize the global area-weighted percentage of extreme winds over each grid cell that occur within 750 km of a cyclone centre in both present-day and warmer climate simulations. The distributions are presented for each grid cell, partitioned by hemisphere and simulation type. In the present-day climate scenario, the median frequency of cyclone-associated wind speed events is comparable in magnitude between the two hemispheres, with 83% in the NH and 88% in the SH. However, the SH distribution exhibits a slightly longer tail towards lower frequencies of cyclone-associated extreme wind speeds compared to the NH. This distinction is likely attributed to the presence of Antarctica's orography, which acts as a barrier shielding the interior landmass points from midlatitude cyclones, resulting in lower occurrence frequencies in the SH.

Spatially, the highest frequency of cyclone-associated extreme wind speed events is concentrated along the major midlatitude storm tracks in both hemispheres, as depicted in Fig. 3b, c. The North Atlantic, North Pacific, and SH storm tracks consistently exhibit between 80% and 100% of cyclone-associated extreme wind speed events, providing objective evidence for the influential role of midlatitude cyclones in driving wind extremes in the midlatitudes, as also demonstrated by a recent global analysis of compound wind and precipitation extremes using ERA5[34].

Under the warmer climate scenario, when considering the total number of midlatitude cyclone tracks obtained using the Hodges'

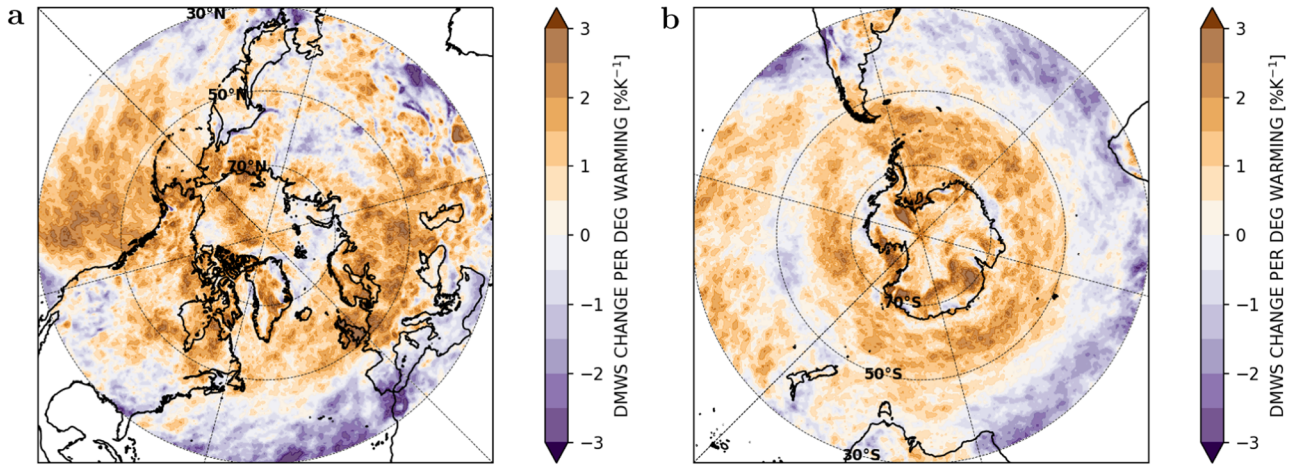

Fig. 2 Map of extreme wind speeds in AM4 idealised warmer climate simulations. Percentage change in the median of the 99th-100th percentiles daily maximum 10-m wind speeds (DMWS), corresponding to the 99.5th percentile $v_{99.5}$, per degree of SST warming for the **a** Northern Hemisphere and **b** Southern Hemisphere.

(1999) algorithm[35], there is a decrease of approximately 4% compared to the present-day climate scenario. However, the examination of the aggregated area-weighted frequency distributions of cyclone-associated events (refer to Fig. 3a), indicates that the medians of their warmer climate distributions increase by approximately 2% in both hemispheres compared to the corresponding present-day values. Nevertheless, a more detailed analysis of the spatial distributions in Fig. 3d, e reveals notable changes. While the frequency of cyclone-associated extreme winds remains relatively constant in the central regions of the midlatitude storm tracks, it decreases closer to the tropical regions and increases towards the poles along the edges of the storm tracks.

These findings indicate a shift towards higher frequencies of cyclone-associated extreme wind speeds in poleward regions (in both hemispheres). In the NH (Fig. 3b–d), the largest shift (increases up to 10%) occur over inhabited areas such as Britain and Scandinavian countries. In the SH (Fig. 3c–e), a substantial shift, comparable in magnitude, (increases up to 8%) is observed in the seas and coastlines surrounding Antarctica. These increases are not uniform across all regions. For example, the Southern Indian Ocean (Fig. 3d) experiences decreases of up to 10% in the frequency of cyclone-associated extreme wind speed events, while the decreases are limited to approximately 2% in the Southern Pacific Ocean.

Poleward increase of cyclone-associated near-surface extreme wind speeds

Although, as discussed earlier, the overall poleward increase in the frequency of cyclone-associated extreme wind speed events suggests a shift in the cyclones tracks and intensity in both hemispheres, a further analysis of the changes in wind speed magnitudes associated with cyclones under a warmer climate is necessary. Towards this aim, we assessed the changes in the intensity of cyclone-associated extreme wind speeds under global warming by computing the percentage differences between the warmer climate and present-day climate simulations of cyclone-associated *v*99.5, normalized per SST degree warming, as shown in Fig. 4.

Figure 4 shows a clear intensification of cyclone-associated extreme wind speeds around the poles. In the NH (Fig. 4a), the most significant intensification occurs over the North Pacific, the British Isles, and Northwestern Europe, with increases in cyclone-associated extreme wind speeds which reaches up to 3% per degree of SST warming (equivalent to approximately 1.5 m s^{-1} in absolute value, not shown) and are concentrated between latitudes 50°N and 70°N. Similarly, in the SH (Fig. 4b), the projected changes in cyclone-associated extreme wind speeds exhibit a more symmetrical pattern compared to the NH, with a roughly homogeneous increase in cyclone-associated extreme wind speeds of approximately 2.5% per degree of SST warming (localized between latitudes 50°S and 70°S) around the Antarctica landmass. In contrast, both hemispheres experience a decrease in the lower midlatitudes of up to 3% per degree of SST warming, between 30°N and 50°N or 30°S and 50°S. The Pacific ocean is the only region in both hemispheres that displays increases in cyclone-associated extreme wind speeds extending to the tropics. These findings mirror the results presented in Fig. 1c, d, indicating that the projected changes in extreme wind speed events under warmer climate conditions can be attributed to the changes in cyclone-associated extreme wind speed events. Additionally, statistical analysis of the distributions of the cyclone-associated extreme wind speeds at each model grid cell shows that they satisfy the Mann-Whitney U test ($p < 0.05$), indicating the statistical significance of the results presented in Fig. 4a, b.

To gain further insights into the physical characteristics of cyclones associated with extreme wind speed events, we examined the mean changes in cyclone track densities and intensities between the warmer and the present-day climate simulations. The results, illustrated in Fig. 5, reveal distinct patterns in terms of changes in cyclone intensity and track density.

Figure 5a–b visually demonstrates that in the warmer climate simulation the cyclone track intensity of midlatitude cyclones associated with extreme wind speed events strengthens near the poles in both hemispheres and weakens as the distance from the poles increases. In the NH (Fig. 5a), the regions of the Atlantic Ocean north of the British Isles and Northern Europe, as well as the northern part of the Pacific Ocean, experience increases in cyclone intensity characterized by relative vorticity at 850 hPa (ξ_{850}) of up to $0.5 \times 10^{-5}\,s^{-1}$. Conversely, the southern parts of the North Atlantic and North Pacific exhibit an equal and opposite decrease in cyclone intensity, reaching values of up to $-0.5 \times 10^{-5}\,s^{-1}$. Shifting our focus to the Southern Hemisphere (Fig. 5b), the changes in cyclone intensity under the warmer climate simulations demonstrate a more symmetric pattern. Poleward increases in cyclone intensity are observed around the Antarctic landmass between 60° and 70°S, reaching maximum values of $0.5 \times 10^{-5}\,s^{-1}$, which are comparable to those found in the Northern Hemisphere. Additionally, reductions in relative vorticity at 850 hPa (ξ_{850}) away from the poles exhibit a symmetric distribution spanning the lower midlatitudes between 30° and 40°S.

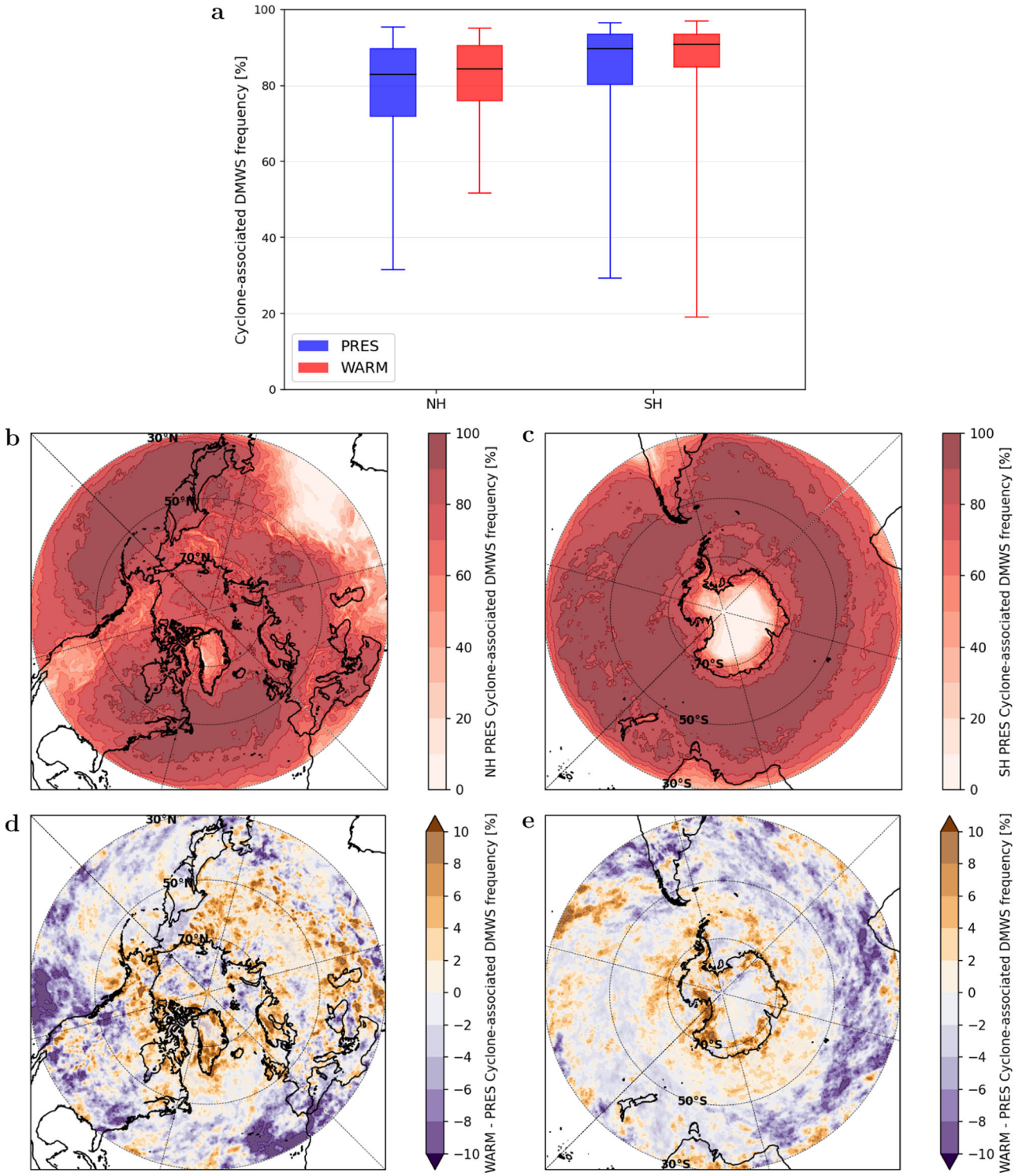

Fig. 3 Cyclone-associated DMWS frequency as aggregated statistics and spatial distribution for present-day and warmer climate. a Box plot of area-weighted cyclone-associated DMWS frequency exceeding the 99th percentile threshold in GFDL-AM4 model for present-day (blue) and warmer climate (red) simulations. Whiskers represent the 0.3 and 99.7% percentiles, box indicates interquartile range, and median, 25th, and 75th percentiles are marked. **b** Northern Hemisphere cyclone-associated DMWS occurrence, **c** Southern Hemisphere cyclone-associated DMWS occurrence, **d** difference between NH warmer and present-day cyclone-associated DMWS frequency, **e** difference between SH warmer and present-day cyclone-associated DMWS frequency.

The comparison of Fig. 5a, b with c, d, which illustrates the changes in track densities of midlatitude cyclones associated with extreme wind speed events in the context of warmer climate conditions, reveals a robust spatial agreement with intensity changes, particularly around the poles. In the SH, the changes in track density of cyclones associated with extreme wind speeds exhibit a relatively homogeneous pattern, characterized by a nearly symmetrical increase in track density. In the NH, the changes in track density of cyclones associated with extreme wind speeds appear more varied. Specifically, the North Atlantic Storm

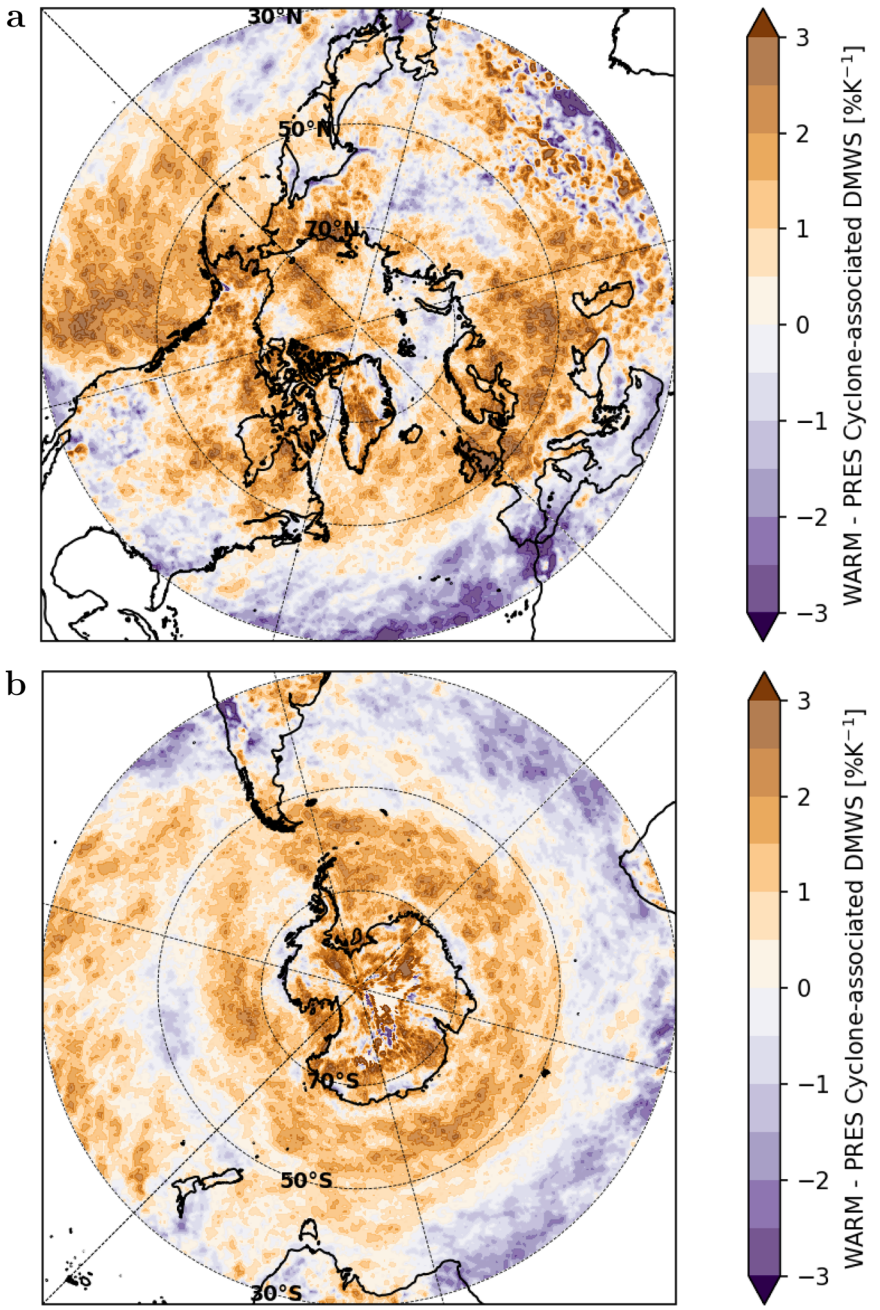

Fig. 4 Map of cyclone-associated extreme wind speeds in AM4 idealised warmer climate simulations. Panels same as in Fig. 2a, b but considering only the median of the 99th-100th percentiles cyclone-associated DMWSs ($v99.5$). **a** Northern Hemisphere and **b** Southern Hemisphere.

track extends further into the British Isles and Northern Europe. On the other hand, the North Pacific storm track experiences a reduction in cyclone track density between the western coast of Canada and Japan within a narrow range of approximately 45°N, but expands over the North Pacific in other areas. Notably, the decrease in track density along this narrow region corresponds to an increase in both cyclone intensity and cyclone-associated extreme wind speeds. This suggests that the intensification of extreme wind speeds is primarily driven by the cyclone intensity itself, as defined here by ξ_{850}, rather than by changes in track density. Lastly, the results presented here are likely to differ across different seasons due to the seasonal variation in the distribution of track density[36].

DISCUSSION

Understanding changes in the pattern and magnitude of extreme wind speeds associated with midlatitude cyclones under a warming climate has great significance for the safety of lives, businesses, and infrastructure. Although it has long been known that midlatitude cyclones lead to extreme wind speeds at the surface, either through individual studies or storm composites[5,37,38], a systematic investigation of their contribution to extreme near-surface wind speed events (also known as cyclone footprint) in both the NH and SH under present-day and warmer climate has been scarce[12]. Here, we investigated the contribution of midlatitude cyclones to changes in extreme wind speed events under an idealised future global warming scenario, obtained

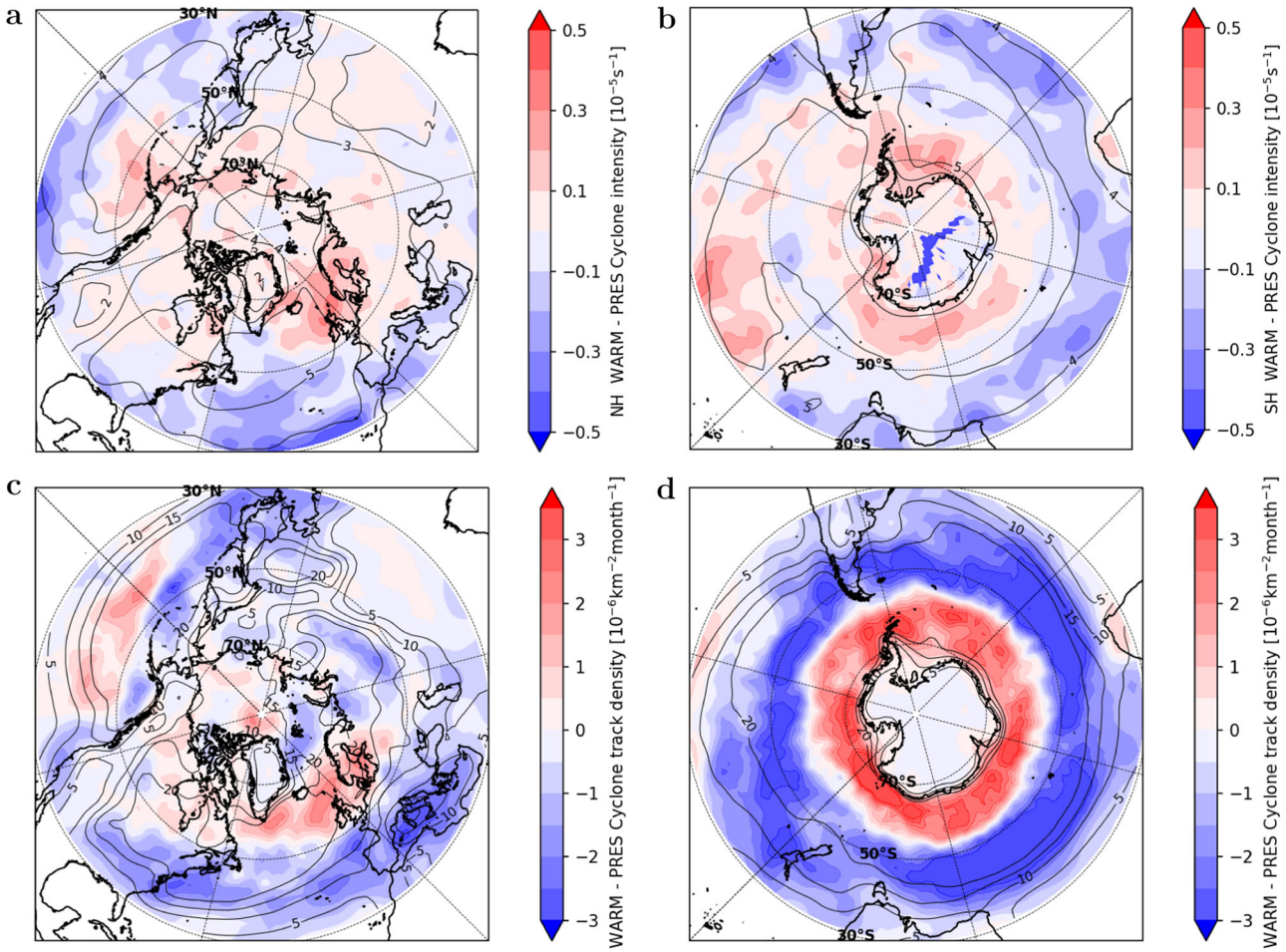

Fig. 5 Map of changes in the midlatitude cyclones track density and intensity associated with extreme wind speeds under idealised warmer climate. Difference in midlatitude cyclone track mean intensity (associated with extreme wind speed events) between the warmer and the present-day climate AM4 simulations for the **a** Northern Hemisphere and the **b** Southern Hemisphere, overlaid present-day climate cyclone track intensity (black contours). Difference in midlatitude cyclone track density (associated with extreme wind speed events) between the warmer and the present-day climate AM4 simulations for the **c** Northern Hemisphere and the **d** Southern Hemisphere, overlaid present-day climate cyclone track density (black contours). Units of track densities are number of cyclones per 5° spherical cap per month.

adding homogeneously 2 K in the SST to a present-day simulation covering the 71-year period of 1949–2019 using the state-of-the art high-resolution ≈ 50 km GFDL climate model AM4.

The results of our objective attribution of extreme wind speed events to midlatitude cyclones demonstrate that midlatitude cyclones account for the vast majority of extreme near-surface wind speed events (between 80% and 100% of the extreme wind speed events) in the regions of the major midlatitude storm tracks, such as the North Atlantic, North Pacific, and the Southern Hemisphere storm tracks. In these regions the median value of the extreme wind speeds consistently exceeds 25 m s^{-1}, which corresponds to the storm-intensity winds and Beaufort scale 10, indicating a potential for significant hazards.

Although, under the idealized global warming scenario, the frequency of cyclone-associated extreme events is roughly unchanged and the number of midlatitude cyclones decreases by roughly 4%, we observed a migration of the cyclone-associated extreme wind speeds in frequency and intensity towards higher latitudes. The spatial distributions of extreme wind speeds simulated by the AM4 model, align well with the changes in the cyclone-associated extreme wind speeds, implying that changes in midlatitude cyclone track density and intensity are the primary drivers of changes in the midlatitude extreme wind patterns. Overall, extreme wind speeds increase by roughly 4% K^{-1} towards the poles, accompanied by an increase in midlatitude cyclone track density of up to 5×10^{-6} km^{-1} s^{-1} and cyclone intensity of up to 0.5×10^{-5}s^{-1} in both the NH and SH. A positive relationship among poleward shift of midlatitude cyclone storm tracks, cyclone intensification, and increase in greenhouse gas emissions (indicative of warmer climate) was also highlighted by a recent assessment of CMIP6 model simulations conducted under various Shared Socio-economic Pathways (SSP1-26, SSP2-45, SSP3-70, and SSP5-85) with a resolution of ≈ 100 km, twice as coarse as the ≈ 50 km employed in our study, and in line with the results from previous CMIP5 assessments concerning the NH[9], and the SH midlatitude storm tracks[39]. Although there is no consensus amongst scientists regarding the exact causes of the poleward shift of midlatitude storm tracks also found in our study, several key underlying physical mechanisms have been identified in assessments of CMIP5 and CMIP6 model ensembles[40,41]. These mechanisms include, but are not limited to, stronger upper-level winds, increased atmospheric water vapor[40], and tropical warming[41]. However, further research is needed to establish the precise link between these mechanisms and the poleward shift of the cyclone-associated near-surface extreme wind speeds demonstrated in our study, while disentangling it from other relevant feedbacks such as the expected increase in static stability under a warmer climate. Overall, although the poleward shift of midlatitude cyclone tracks has been amply discussed in the literature, its extension to cyclone-associated near-surface extreme wind

speeds, demonstrated in our study, represents an important result, for a twofold reason: (1) for its significance, being driven in our study solely by the global mean anthropogenic warming represented by the prescribed +2K SST, and (2) for the research methods used, which combines an intermediate complexity simulation framework with an Eulerian analysis of the cyclone-associated extreme wind speeds.

The regions most significantly affected, in our study, by the poleward migration of midlatitude cyclones and the resulting increase in cyclone-associated extreme wind speeds (up to 3%K^{-1}) are the British Isles, Northwestern Europe, and the North American west coast. These results confirm, for the British Isles and Europe, the increase in cyclone-associated 850hPa winds found in CMIP5 model ensembles under the midrange and high-emission Representative Concentration Pathway RC4.5 and RC8.5[9]. Notably, according to idealized warmer climate simulations conducted using the AM4 model in a different study[25], the British Isles, Northwestern Europe, and the North American west coast are also projected to experience an increase by as much as 6% K^{-1} in the cyclone-associated extreme precipitation, defined as exceeding the climatological 99th percentile. These regions have already been identified at risk of compound wind and precipitation extremes driven by midlatitude-cyclones in the present climate[34], and compound coastal flooding under warmer climate, the latter compound hazard frequency being projected to increase by ≈ 2.5 times than in the present-day climate for latitudes above 40°[42]. Consequently, in light of the results of our study and of previous findings, the British Isles, Northwestern Europe, and the Western Coast of North America turn out as the inhabited areas most vulnerable to a heightened risk of compound wind, precipitation, and coastal flooding hazards under a warmer climate. This is in contrast to the SH midlatitudes, where the limited presence of populated areas reduces the potential impacts of increased frequency of climate extremes. Future research on climate projections of compound extreme wind speeds and precipitation hazards should prioritize the quantification of risks associated with midlatitude cyclones, taking into account the findings of our study, which specifically examines extreme wind speeds, recent results from future projections of compound precipitation and coastal flooding extremes based on CMIP simulations[42], as well as present-day reanalysis-based analyses like ERA5[34].

When interpreting the estimations of the poleward-increase in cyclone-associated near-surface extreme wind speed presented in our study, two caveats have to be mentioned. Firstly, the use of uniform sea surface temperature (SST) warming may not fully capture the complex effects of regional SST warming patterns[43]. Regional SST patterns can directly influence the locations and intensities of cyclone tracks. As emphasized in recent studies[44,45], incorporating SST warming patterns that increase SST gradients in key cyclogenesis regions, such as the Gulf of Mexico or the Pacific Ocean region influenced by the Kuroshio Current, has the potential to amplify the poleward shift and intensification of midlatitude cyclone tracks. Additionally, accounting for SST warming patterns may also result in regional changes in the occurrence of tropical cyclones transitioning to midlatitude cyclones and subtropical cyclones, which often extend well beyond the tropics[6]. Although our study filters out cyclones with a genesis region in the tropics (between ± 30°), it is likely that the increase in extreme wind speeds observed in the Pacific Ocean, closer to the tropics in the warmer climate simulation, is influenced by a combination of an increased number of hybrid cyclones and a poleward shift of tropical storm genesis regions[46]. Secondly, the AM4 simulations employed in our study do not consider the anticipated decline in sea-ice cover throughout the 21st century[47], resulting from a warmer climate. Consequently, keeping the sea-ice concentration fixed and uniformly adding 2 K to the SST to simulate warmer climate conditions might lead to an artificially enhanced zone of baroclinicity at the sea-ice edge, as the local SST gradients are strongly enhanced, possibly affecting the poleward shift of extreme wind speeds associated to cyclones. In fact, more realistically, in a future warmer climate, surface baroclinicity would likely decrease around the sea-ice edge, as polar regions warm more strongly than the tropics (an effect known as Arctic Amplification in the NH), likely leading to the weakening of the upper-level westerlies[48,49], through the thermal wind relation. This may, in turn, potentially decrease the frequency and strength of midlatitude cyclones, which grow over baroclinic instabilities, particularly in the NH, where sea-ice loss is projected to be most pronounced. On the contrary, some existing literature suggests that incorporating reduced sea ice conditions in high-resolution climate simulations would likely amplify the poleward shift of cyclone-associated extreme wind speeds discussed here for the NH[12,50]. Moreover, a recent study analysing the effect of Arctic sea-ice loss on extratropical cyclones found changes to be small compared to the climate internal variability, though statistically significant, indicating that sea-ice loss represents just one of the many important aspects of the global warming response of midlatitude cyclones, which range from expected changes in atmospheric stability, to latent heating, and vertical stability[51]. Finally, due to the complexity of factors affecting midlatitude cyclones genesis and life-cycle, it remains challenging to project the impact of sea-ice changes on midlatitude cyclone storm tracks under warmer climate[12,48], and further research would be needed to ascertain the role of sea-ice loss on the poleward intensification of cyclone-associated near surface extreme wind speeds.

Future research could focus on conducting more km-scale global climate simulations to obtain more precise regional estimates regarding the poleward migration of cyclone-associated extreme wind speeds[52], particularly in densely populated areas of the British Isles, Northwestern Europe, and the West Coast of the US and Canada. Enhanced understanding in this regard would be invaluable for informing strategies to mitigate the potential impacts of extreme wind events in vulnerable regions[53]. Furthermore, these simulations could delve into the mesoscale features of midlatitude cyclones that contribute to surface-level extreme wind speed events, expanding upon the results of regional studies conducted for instance over the British Isles[54]. By examining both present-day and warmer-climate scenarios, these investigations could yield more detailed understanding of the underlying dynamics and atmospheric conditions that give rise to extreme wind speed events.

METHODS

Model

The climate model used in the study is the latest high-resolution version of the GFDL atmospheric climate model (AM4). It employs a cubed-sphere topology for its atmospheric dynamical core with 192 × 192 grid boxes per cube face corresponding to roughly 50-km horizontal grid spacing. This GFDL atmospheric climate model versions, AM4, has been used for GFDL's participation in the CMIP6 High Resolution Model Intercomparison Project[18,25].

To investigate the projected changes in wind speeds under human-induced global warming the AM4 model was run for a present day and a future climate idealised global-warming simulation, with a homogeneous SST increase of 2K. Details of the present-day and future warmer climate simulations are now given:

- Present-day simulation. The present-day simulation is a climate integration of the 71-year period of 1949–2019. The model is forced by the observed daily SSTs, sea ice concentrations, and radiative gases following the CMIP6 HighResMIP specifications[18].
- Future warmer climate simulation. The future warmer climate

simulation is an idealized global-warming experiment that is the same 71-year climate integration as the present-day simulation but with observed daily SSTs uniformly increased by 2 K. The warming simulation is used to explore the possible change in midlatitude-cyclones-associated extreme wind speeds in a future warmer climate.

Midlatitude cyclones tracking

The cyclone tracking was carried out using Hodges' algorithm (1995)[35]. To identify cyclones, the algorithm employs the 6-hourly relative vorticity at 850 hPa, ξ_{850}, as an input. The use of relative vorticity at the 850 hPa level is advantageous for detecting cyclones in the lower troposphere compared to mean sea level pressure. It enables early identification of cyclone systems and is less influenced by large-scale background effects, as ξ_{850} focuses on the smaller-scale synoptic range compared to mean sea level pressure[55].

Initially, the algorithm spectrally truncates the relative vorticity field to T42 resolution. This step is necessary since a high-resolution relative vorticity field ($\approx$ 50 km grid-spacing in AM4 configurations used in our study) tends to exhibit significant noise, making it less suitable for tracking purposes. To remove the influence of planetary scale waves, the algorithm masked wavenumbers $\leq$5.

Subsequently, the algorithm performs the tracking process by first initialising a set of tracks from the feature points and then refining the tracks by minimizing a cost function, which aims to achieve a smoother ensemble of tracks. The positive and negative anomalies in ξ_{850}, corresponding to cyclones in the Northern Hemisphere (NH) and the Southern Hemisphere (SH) respectively, were tracked separately. Importantly, the tracking operates on a spherical domain, eliminating the need for projections that may introduce systematic biases. This approach allowed for the analysis of global data or large spherical regions.

Furthermore, the algorithm retained only those tracks from the ensemble of tracks that persisted for at least 48 hours and traveled a minimum distance of 1000 km from the cyclone points of origin. This criterion ensured that only mobile, well-developed, and long-lived cyclones were included in the analysis. Additionally, each cyclone was required to exhibit a maximum vorticity of at least 1×10^{-5} s^{-1} (scaled by -1 in the SH).

To derive spatial statistics, spherical kernel methods[56] were employed on the track ensembles directly on the unit sphere. This approach was chosen to avoid the biases of grid box methods and map projections. Furthermore, the initial identification of cyclone centers before tracking is performed on a polar projection to mitigate any latitudinal bias introduced by the meridian convergence near the poles[30,56].

It is important to note that the choice of a tracking method based on different meteorological fields, such as Mean Sea Level Pressure (MSLP), is likely to yield different cyclone track density patterns. This divergence primarily arises because various tracking methods do not consistently identify the same weather systems. For example, a comprehensive intercomparison study of different midlatitude cyclone detection and tracking algorithms that used both relative vorticity and MSLP[57] revealed that cyclones tracked using a relative vorticity-based approach, similar to the method employed in our study, tend to be displaced poleward compared to those tracked using pressure-based methods. However, it is worth noting that when focusing exclusively on deep cyclones, which are the ones most likely to generate extreme near-surface wind speeds (the primary focus of this paper), the disparities in tracks produced by relative-vorticity and pressure-based methods exhibit better agreement, as demonstrated in the same inter-comparison study[57].

Determining cyclone-associated extreme-wind speeds

Extreme wind speeds were defined as those exceeding the 99th percentile of the daily maximum 10-m surface wind speed, separately for the present and warmer climate experiments, and thus characterize the upper (or extreme) tail of the wind speed distribution at each model grid cell over the globe in each climate simulation performed. Considering only Daily Maximum Wind Speeds (DMWS) allowed to select only independent extreme wind speed events. An objective approach was used to associate extreme wind speeds and midlatitude cyclones by defining each DMWS event that exceeded the 99th percentile threshold as cyclone-associated if it was within a 750-km radius of the nearest midlatitude cyclone track point. The midlatitude cyclone track point had to match the time of the DMWS event to the nearest 6-hour interval. We performed some sensitivity analysis to determine the robustness of our findings to the radius size and found that changes of $\pm$ 50 km led to changes of only roughly $\pm$ 1% in the frequency of cyclone-associated events. This method has been used by a few recent studies to objectively and systematically associate modelled[58] and observed[59] extreme wind speed events to midlatitude cyclones.

DATA AVAILABILITY

The ERA5 data by the European Centre for Medium-Range Weather Forecast (ECMWF) are available at https://cds.climate.copernicus.eu/cdsapp#!/dataset/reanalysis-era5-single-levels. The GFDL-AM4 model simulation outputs analysed in this study are available from the corresponding authors upon reasonable request.

CODE AVAILABILITY

The GFDL-AM4 model is available at https://github.com/NOAA-GFDL/AM4. Codes used for analysis are available from the corresponding author upon reasonable request.

Received: 15 June 2023; Accepted: 29 November 2023;
Published online: 21 December 2023

REFERENCES

1. Munich Re. Winter storms in Europe (II) - Analysis of 1999 losses and loss potentials. Munich Reinsurance Group. Munich. (2002).
2. Swiss Re. Natural catastrophes and man-made disasters in 2010: a year of devastating and costly events. Sigma. No 1/2011. "https://www.swissre.com/dam/jcr:d58dea24-f966-4614-8b90-3acd9b0a361f/sigma1_2011_en.pdf " (2011).
3. Roberts, J. F. et al. The XWS open access catalogue of extreme European wind-storms from 1979 to 2012. *Nat. Hazards Earth Syst. Sci.* **14**, 2487–2501 (2014).
4. Letson, F. W., Barthelmie, R. J., Hodges, K. I. & Pryor, S. C. Intense windstorms in the northeastern United States. *Nat Hazards Earth Syst. Sci.* **21**, 2001–2020 (2021).
5. Hewson, T. D. & Neu, U. Cyclones, windstorms and the IMILAST project. *Tellus A* **67**, 27–128 (2015).
6. Bengtsson, L., Hodges, K. & Keenlyside, N. Will extratropical storms intensify in a warmer climate? *J. Clim.* **22**, 2276–2301 (2009).
7. Pinto, J., Karremann, M., Born, K., Della-Marta, P. & M, K. Loss potentials associated with European windstorms under future climate conditions. *Clim. Res.* **54**, 1–20 (2012).
8. Ulbrich, U. et al. Are greenhouse gas signals of Northern Hemisphere winter extra-tropical cyclone activity dependent on the identification and tracking algorithm? *Meteorol. Z* **22**, 61–68 (2013).
9. Zappa, G., Shaffrey, L. C., Hodges, K. I., Sansom, P. G. & Stephenson, D. B. A multimodel assessment of future projections of North Atlantic and European extratropical cyclones in the CMIP5 climate models. *J. Clim.* **26**, 5846–5862 (2013).
10. Feser, F. et al. Storminess over the North Atlantic and Northwestern Europe: a review. *Q. J. R. Meteorol. Soc.* **141**, 350–382 (2015).
11. Wang, J., Kim, H.-M. & Chang, E. K. M. Changes in Northern Hemisphere winter storm tracks under the background of Arctic amplification. *J. Clim.* **30**, 3705–3724 (2017).
12. Catto, J. et al. The future of midlatitude cyclones. *Curr. Clim. Change* **5**, 407–420 (2019).
13. Priestley, M. D. K. & Catto, J. L. Future changes in the extratropical storm tracks and cyclone intensity, wind speed, and structure. *Weather Clim. Dynam.* **3**, 337–360 (2022).

14. Chang, E. Projected significant increase in the number of extreme extratropical cyclones in the Southern Hemisphere. *J. Clim.* **30**, 4915–4935 (2017).
15. Bengtsson, L., Hodges, K. I. & Roeckner, E. Storm tracks and climate change. *J. Clim.* **19**, 3518–3543 (2006).
16. Harvey, B. J., Cook, P., Shaffrey, L. C. & Schiemann, R. The response of the Northern Hemisphere storm tracksand jet streams to climate change in the CMIP3, CMIP5, and CMIP6 climate models. *J. Geophys. Res.-Atmos.* **125**.
17. Büeler, D. & Pfahl, S. Potential vorticity diagnostics to quantify effects of latent heating in extratropical cyclones. Part II: Application to idealized climate change simulations. *J. Atmos. Sci.* **76**, 1885–1902 (2019).
18. Haarsma, R. J. et al. High resolution model intercomparison project (HighResMIP v1.0) for CMIP6. *Geosci. Model Dev.* **9**, 4185–4208 (2016).
19. Pfahl, S., O'Gorman, P. & Singh, M. Extratropical cyclones in idealized simulations of changed climates. *J. Clim.* **28**, 9373–92.
20. Martínez-Alvarado, O. et al. Increased wind risk from sting-jet windstorms with climate change. *Environ. Res. Lett.* **13** (2018).
21. Manning, C., Kendon, E., Fowler, H. & Roberts, N. Projected increase in windstorm severity and contribution from sting jets over the UK and Ireland. *Weather Clim. Extremes* **40**, 1–15 (2023).
22. Sinclair, V. A., Rantanen, M., Haapanala, P., Räisänen, J. & Järvinen, H. The characteristics and structure of extra-tropical cyclones in a warmer climate. *Weather Clim. Dyn.* **1**, 1–25 (2020).
23. Pryor, S. & Barthelmie, R. Climate change impacts on wind energy: a review. *Renew. Sustain. Energy Rev.* **14**, 430–437 (2010).
24. Pryor, S. & Barthelmie, R. A global assessment of extreme wind speeds for wind energy applications. *Nat Energy* **6**, 268–276 (2021).
25. Zhao, M. et al. The GFDL global atmosphere and land model AM4.0/LM4.0: 2. Model description, sensitivity studies, and tuning strategies. *J. Adv. Model. Earth Syst.* **10**, 735–769 (2018).
26. Zhao, M. A study of AR-, TS-, and MCS-associated precipitation and extreme precipitation in present and warmer climates. *J. Clim.* **35**, 479 – 497 (2022).
27. Cess, R. et al. Intercomparison and interpretation of climate feedback processes in 19 atmospheric general circulation models. *Geophys. Res. Lett.* **95**, 16601–16615 (1990).
28. Dacre, H. & Gray, S. The spatial distribution and evolution characteristics of North Atlantic cyclones. *Mon. Weather Rev.* **137**, 99–115 (2009).
29. Zappa, G. et al. Extratropical cyclones and the projected decline of winter Mediterranean precipitation in the CMIP5 models. *Clim. Dyn.* **45**, 1727–1738 (2015).
30. Hodges, K. I. Feature tracking on the unit sphere. *Mon. Weather Rev.* **123**, 3458–3465 (1995).
31. Hersbach, H. et al. The ERA5 global reanalysis. *Q. J. R. Meteorol. Soc.* **146**, 1999–2049 (2020).
32. Molina, M. O., Gutiérrez, C. & Sánchez, E. Comparison of ERA5 surface wind speed climatologies over Europe with observations from the HadISD dataset. *Q. J. R. Meteorol. Soc.* **144**, 943–969 (2021).
33. Pryor, S., Schoof, J. & Barthelmie, R. Winds of change? Projections of near-surface winds under climate change scenarios. *Geophys. Res. Lett.* **33** (2006).
34. Messmer, M. & Simmonds, I. Global analysis of cyclone-induced compound precipitation and wind extreme events. *Weather Clim. Extrem.* **32**, 100324 (2021).
35. Hodges, K. I. Adaptive constraints for feature tracking. *Mon. Weather Rev.* **127**, 1362–1373 (1999).
36. Hoskins, B. J. & Hodges, K. I. The annual cycle of Northern Hemisphere storm tracks. Part I: Seasons. *J. Clim.* **32** (2019).
37. Parton, G. A., Dore, A. & Vaughan, G. A climatology of mid-tropospheric mesoscale strong wind events as observed by the MST radar, Aberystwyth. *Meteor. Appl.* **17**, 340–354 (2010).
38. Martínez-Alvarado, S. O., Gray, S. L., Catto, J. L. & Clark, P. A. Sting jets in intense winter North-Atlantic windstorms. *Environ. Res. Lett.* **7**, 1–8 (2012).
39. Chang, E., Guo, Y. & Xia, X. CMIP5 multimodel ensemble projection of storm track change under global warming. *J. Geophys. Res. Atmos.* **117**, 1–19 (2012).
40. Tamarin-Brodsky, T. & Kaspi, Y. Enhanced poleward propagation of storms under climate change. *Nat. Geosci.* **10**, 908–913 (2017).
41. Oudar, T., Cattiaux, J. & Douville, H. Drivers of the northern extratropical eddy-driven jet change in CMIP5 and CMIP6 models. *Geophys. Res. Lett.* **47** (2020).
42. Bevacqua, E. et al. More meteorological events that drive compound coastal flooding are projected under climate change. *Commun. Earth Environ.* **1**, 47 (2020).
43. Villarini, G. & Vecchi, G. A. Twenty-first-century projections of North Atlantic tropical storms from CMIP5 models. *Nat. Clim. Change* **2**, 604–607 (2012).
44. Brayshaw, D. J., Hoskins, B. & Blackburn, M. The storm-track response to idealized SST perturbations in an aquaplanet GCM. *J. Atmos. Sci.* **65**, 2842–2860 (2008).
45. Graff, L. S. & LaCasce, J. H. Changes in cyclone characteristics in response to modified SSTs. *J. Clim* .**27**, 4273–4295 (2014).
46. Liu, M., Vecchi, G., Smith, J. & Murakami, H. The present-day simulation and twenty-first-century projection of the climatology of extratropical transition in the North Atlantic. *J. Clim.* **30**, 2739–2756 (2017).
47. Stroeve, J. et al. Trends in Arctic sea ice extent from CMIP5, CMIP3 and observations. *Geophys. Res. Lett.* **39**, 1–7 (2012).
48. Shaw, T. A. & Voigt, A. Understanding the links between subtropical and extratropical circulation responses to climate change using aquaplanet model simulations. *J Clim* **29**, 6637 – 6657 (2016).
49. Smith, D. et al. Robust but weak winter atmospheric circulation response to future Arctic sea ice loss. *Nat. Commun.* (2022).
50. Bader, J. et al. A review on Northern Hemisphere sea-ice, storminess and the North Atlantic Oscillation: observations and projected changes. *Atmos. Res.* **101**, 809–834 (2011).
51. Hay, S., Priestley, M., Hao, Y., Catto, J. L. & James, A. The effect of Arctic sea-ice loss on extratropical cyclones. *Geophys Res. Lett.* **50**, 1–11 (2023).
52. Priestley, M. & Catto, J. Improved representation of extratropical cyclone structure in HighResMIP models. *Geophys. Res. Lett.* **49**, 1–10 (2022).
53. Slingo, J. et al. Ambitious partnership needed for reliable climate prediction. *Nat. Clim. Chang* **12**, 499–503 (2022).
54. Manning, C. et al. Extreme windstorms and sting jets in convection-permitting climate simulations over Europe. *Clim. Dyn.* **58**, 2387–2404 (2022).
55. Chang, E. K. M. Impacts of background field removal on CMIP5 projected changes in Pacific winter cyclone activity. *J. Geophys. Res. Atmos.* **119**, 4626–4639 (2014).
56. Hodges, K. I. Spherical nonparametric estimators applied to the UGAMP model integration for AMIP. *Mon. Weather Rev.* **124**, 2914 – 2932 (1996).
57. Neu, U. et al. IMILAST: A community effort to intercompare extratropical cyclone detection and tracking algorithms. *Bull Am. Meteorol. Soc.* **94**, 529 – 547 (2013).
58. Hart, N. C. G., Gray, S. L. & Clark, P. A. Sting-jet windstorms over the North Atlantic: climatology and contribution to extreme wind risk. *J. Clim.* **30**, 5455–5471 (2017).
59. Gentile, E. & Gray, S. Attribution of observed extreme marine wind speeds and associated hazards to midlatitude cyclone conveyor belt jets near the British Isles. *Int. J. Climatol.* **43**, 2735–2753 (2023).

ACKNOWLEDGEMENTS

This research was jointly funded as part of a Climate Process Team (CPT) under Grant AGS-1916689 from the National Science Foundation and Grant NA19OAR4310363 from the National Oceanic and Atmospheric Administration.

AUTHOR CONTRIBUTIONS

E.S.G.: Conceptualization; formal analysis; method; writing original draft; writing-review and editing. M.Z.: Conceptualization; data curation; method; funding acquisition; supervision. K.H. Conceptualization; Method.

COMPETING INTERESTS

The authors declare no competing interests.

ADDITIONAL INFORMATION

Correspondence and requests for materials should be addressed to Emanuele Silvio Gentile.

Reprints and permission information is available at http://www.nature.com/reprints

Publisher's note Springer Nature remains neutral with regard to jurisdictional claims in published maps and institutional affiliations.